Communications

A New Heuristic Geometrical Approach for Finding Non-Coplanar Multiple Edge Diffraction Ray Paths

K. H. Ng, E. K. Tameh, and A. R. Nix

***Abstract*—Rooftop diffraction can contribute significantly to the propagation path loss in outdoor microcellular environments. For non-coplanar multiple edges, the finding of exact ray paths requires a complex algebraic analysis that is infeasible for rapid application in deterministic ray tracing models. A new heuristic geometrical approach is reported that finds the ray paths for arbitrary height rooftop diffraction and rooftop-to-building corner diffraction. This method can be applied to any 3-D image based ray tracing model. The accuracy of the new method is first quantified using two specific test cases. The method is then implemented in an existing microcellular ray model and path loss predictions are compared with measured data. The heuristic diffraction approach is shown to be simple to implement and lowers the prediction error when compared with the traditional Vertical Plane diffraction approximation.**

***Index Terms*—Diffraction, propagation, ray tracing.**

I. Introduction

High frequency electromagnetic wave propagation modelling using the geometrical optics (GO) approach has allowed the advancement of efficient deterministic ray tracing models for the analysis of wireless propagation channels [1]. The process of ray tracing can be broken down into two stages, 1) ray path identification and 2) electromagnetic modelling. Ray path identification is the process of finding possible ray paths between the transmitter (Tx) and receiver (Rx). A ray path is a poly-line that describes the ray optical route between the Tx and Rx, including interactions with the environment. Electromagnetic modelling then applies various approximated high frequency models, such as the GO Fresnel reflection model and the uniform theory of diffraction (UTD) for each propagation mechanism in order to calculate the field strength at the Rx [2], [3]. Although numerical full-wave solutions such as the method of moments (MoM), finite-difference time-domain (FDTD), and some hybrid MoM/UTD models can account for complex electromagnetic propagations (including multiple diffraction), their scope is restricted to much smaller structures (in terms of wavelength) [4].

According to Keller's geometrical theory of diffraction (GTD), from the generalized Fermat's principle, diffraction at an edge produces a cone of diffracted rays, known as Keller's cone [2]. Keller's cone has its semi-angle equal to the incident angle of the ray. In the case of normal incidence, the cone reduces to a disc. For multiple edge diffraction, when two consecutive diffraction edges are non-coplanar, i.e., when the edge orientations and the heights are different, the finding of the diffraction points cannot be determined efficiently using a simple geometric approach [3], [5], [6]. The exact solution requires complex mathematical computations that are not viable for rapid application in ray tracing models [7], [8]. An efficient solution to the multiple edge diffraction problem is thus restricted to the special case of coplanar diffraction (where the edges form a flat plane), which includes same-height (rooftop) diffraction and multiple vertical edge (building corner) diffraction. In outdoor propagation environments, rooftop multiedge diffractions may contribute significantly to the total signal power and in most cases these diffraction edges do not form a flat plane due to differences in building heights [9], [10]. As a result, multiple rooftop diffraction is usually i) omitted; ii) approximated by vertical plane diffraction; or iii) restricted to the special case of same-height rooftop diffraction [6], [11]. In this paper, an efficient heuristic geometrical approach to solve arbitrary height rooftop and rooftop-to-building corner multiple edge diffraction is presented.[1] This method is particularly suitable for image-based ray tracing, and thus differs from the approximate technique reported in [8], which uses a ray sampling method that is well suited to forward ray tracing (ray launching).

Manuscript received October 21, 2004; revised February 17, 2006. The work of K. H. Ng was supported in part by the IST-2001-32549 ROMANTIK project.

The authors are with the University of Bristol, Bristol BS1 1UB, U.K. (e-mail: k.h.ng@bris.ac.uk; tek.tameh@bris.ac.uk; andy.nix@bris.ac.uk).

Digital Object Identifier 10.1109/TAP.2006.880775

II. New Heuristic Geometrical Approach

The heuristic path finding approach is based on two key diffraction principles: 1) the rotated diffraction image lies on a circular locus and 2) the perpendicular projection of the image for subsequent diffraction [5]. A generic double edge diffraction scenario consisting of a Tx/Rx pair, two diffraction edges, E_1 and E_2, and two diffraction points, D_1 and D_2, is shown in Fig. 1(a). First, the loci of the rotated diffraction images I_1 and I_2 are computed (steps 1–4), and secondly back tracing is used to determine D_1 and D_2 (step 5). The key steps are summarized below.

1) As shown in Fig. 1(b), the rotated diffraction image I_1 is constrained to lie on a circular locus perpendicular to edge E_1 with center C_1 and a radius L_1 (given by the perpendicular distance from Tx to edge E_1).

2) As shown in Fig. 1(c), point C_2 is calculated as the perpendicular projection of point C_1 onto edge E_2.

3) The perpendicular distance from C_1 to C_2 is added to L_1 to form the distance L_2.

4a) In the case of coplanar diffractions, the circular locus of the rotated diffraction image I_2 will be perpendicular to E_2 with center C_2 and radius L_2.

4b) In the case of non-coplanar diffractions, the circular locus of the rotated image I_2 is now found in a heuristic manner. As shown in Fig. 1(c), a plane P_1 is defined by point C_2 and edge E_1. Point X is defined by the intersection of the circular locus of I_1 with plane P_1. In practice, two intersection points exist, one on either side of edge E_1. X is chosen as the intersection that maximizes the distance from C_2. As shown in Fig. 1(d), the circular locus of the rotated diffraction image I_2 will be perpendicular to E_2 with center C_2' and radius L_2'. C_2' is determined from the perpendicular projection of X onto edge E_2. It should be noted that our heuristic step results in $\mathrm{C}_2' = \mathrm{C}_2$ and $\mathrm{L}_2' = \mathrm{L}_2$ in the case of coplanar diffraction.

5) Given the loci of the rotated diffraction images and knowledge of the Rx location, standard back-tracing [5] is performed to find diffraction points D_1 and D_2. D_2 is found as the intersection of the diffraction edge E_2 and a line connecting the Rx with the locus of the rotated diffraction image I_2. D_1 is found as the intersection

[1] A complete study of efficiency would include other computational costly factors such as the ray object shadowing tests.

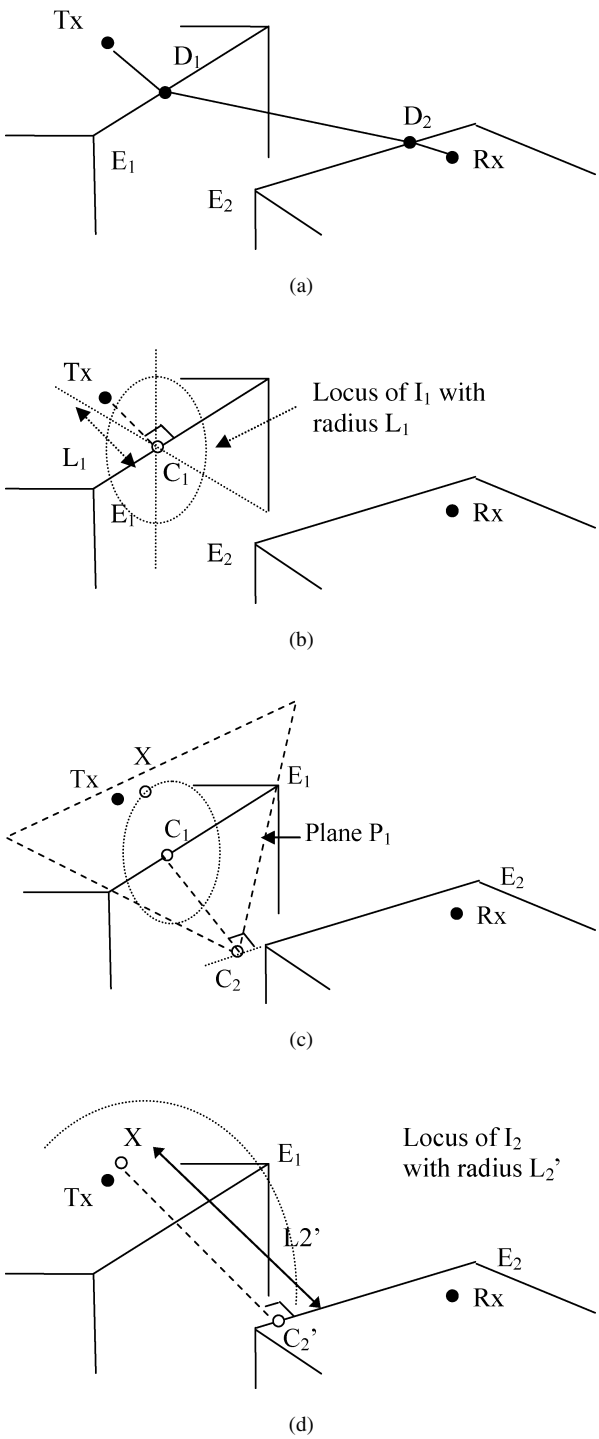

Fig. 1. (a) Double diffraction scenario. (b) Creation of first rotating diffraction image. (c) Before creation of second diffraction image. (d) Creation of second rotating diffraction image.

of the diffraction edge E_1 and a line connecting D_2 with the locus of the rotated diffraction image I_1.

III. Evaluation With Test Model

In order to evaluate the error associated with our new heuristic solution when applied to multiple rooftop and rooftop-to-building

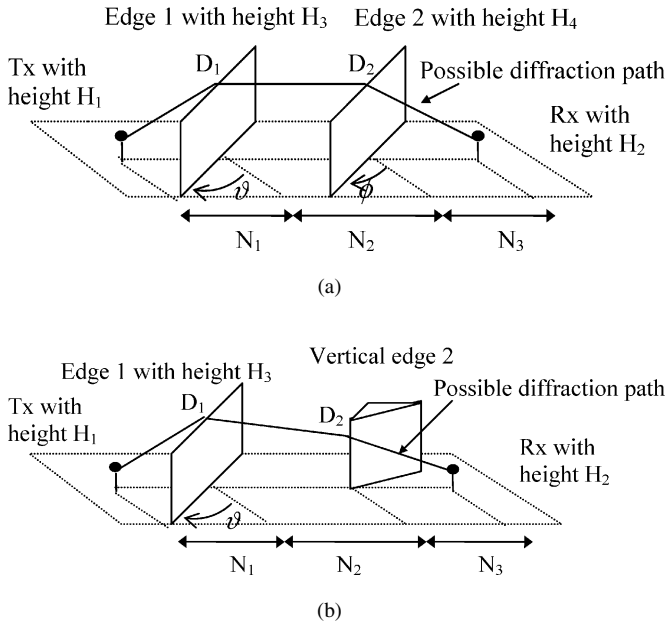

Fig. 2. Test model for (a) arbitrary height rooftop diffraction (HH) and (b) roof-top building corner diffraction (HV).

corner (vertical edge) diffraction, two test models were created as shown in Fig. 2(a) and (b). The first model (HH) consists of two horizontal diffraction edges with heights H3 and H4, a Tx point of height H1 and an Rx point of height H2. ϑ and ϕ represent the horizontal rotation angles for diffraction edges 1 and 2, respectively. N1, N2, and N3 are defined in Fig. 2(a) as the respective distance gaps along the main axis connecting the Tx and Rx. The second model (HV) is similar to the first, except that the second diffraction edge is now vertical. Simulations were implemented with 1,000,000 random (uniformly distributed) data sets for the model parameters, such that: $\mathrm{N1}, \mathrm{N2}, \mathrm{N3} \in (0, 1000m)$ and $\mathrm{H1}, \mathrm{H2}, \mathrm{H3}, \mathrm{H4} \in (0, 100m)$. These data extents were considered typical for microcellular applications. The difference between the incident $(\Delta_{\mathrm{Incident}})$ and diffraction $(\Delta_{\mathrm{Diffraction}})$ angles and the total ray path lengths using our approximate method $(\mathrm{P}_{\mathrm{image}})$ and the ray sampling method described in [7] $(\mathrm{P}_{\mathrm{sampling}})$ was computed. The results of the ray sampling method are generated to be close to the exact solution (i.e., for this method the difference between the incident and diffraction angles is less than 1°).

Table I shows a summary of these comparisons. The angular error term is defined as $\Delta_{\mathrm{Error}} = \mathrm{mean}(|\Delta_{\mathrm{Incident}} - \Delta_{\mathrm{Diffraction}}|)$. The ray path length error term is defined as $\mathrm{P}_{\mathrm{Error}} = |\mathrm{P}_{\mathrm{image}} - \mathrm{P}_{\mathrm{sampling}}|/\mathrm{P}_{\mathrm{sampling}}$. The ray path length error is seen to be negligible. When the two diffraction edges are close to being coplanar (i.e., in the case of ϑ, $\phi \in (\pm 15^0)$), the angular error tends to zero. Assuming an angular error tolerance of 10°, and for edge angles restricted to $\pm 45^\circ$, the HH and HV tests led to acceptable heuristic results for 85% and 96% of the 1,000,000 configurations analyzed. Larger errors in the HH model were seen when both edge angles were close to their maximum value (and of opposite polarity). According to UTD, horizontal diffractions only contribute significantly when the diffraction horizontal rotation angle (ϑ and ϕ) is small [2]. We can therefore conclude that for all significant diffraction cases (and for the vast majority of all other cases), the heuristic algorithm provides an accurate result. It should be noted that in complex UTD-based models, multiple diffractions (beyond second order) are usually omitted since either become invalid or they fail to contribute significantly to the received power.

TABLE I
STATISTICAL SUMMARY OF TEST MODEL COMPARISON

	Mean Δ_{Error} (^{0})	Std. Dev Δ_{Error} (^{0})	Mean P_{Error}	Std. Dev P_{Error}
HH, ϑ, $\phi \in (\pm 15^0)$	0.59	0.60	0	0
HH, ϑ, $\phi \in (\pm 45^0)$	4.65	3.82	0.003	0.003
HH, ϑ, $\phi \in (\pm 85^0)$	4.76	5.64	0.003	0.003
HV, $\vartheta \in (\pm 45^0)$	1.72	4.42	0.002	0.013
HV, $\vartheta \in (\pm 85^0)$	1.95	4.95	0.002	0.013

TABLE II
STATISTICAL SUMMARY OF PATH LOSS PREDICTION COMPARISON

	Heuristic diffraction	Vertical Plane model
Mean Error (dB)	3.53	4.48
Std. Deviation (dB)	3.11	3.77
Correlation	0.85	0.80

Fig. 3. Trial map of a 1 km × 1 km area in city of Bristol. (Color version available online at http://ieeexplore.ieee.org.)

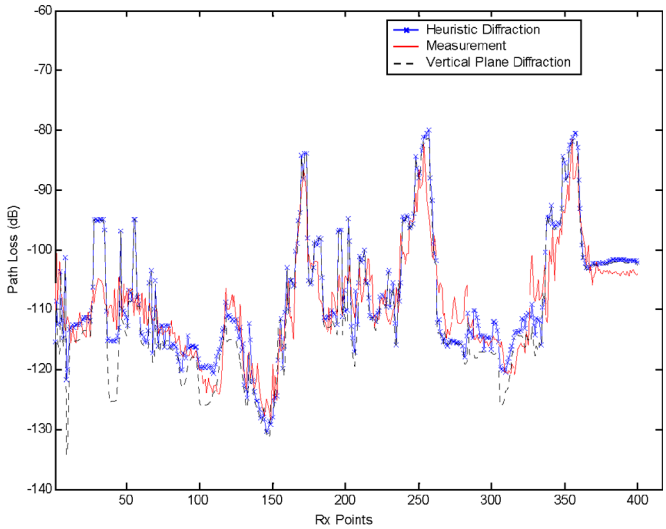

Fig. 4. Path loss prediction comparison of ray tracing models with measurement. (Color version available online at http://ieeexplore.ieee.org.)

IV. COMPARISION WITH MEASUREMENTS

In this section we show that the heuristic diffraction approach is a better approximation than the commonly used vertical plane model. We also show that the new algorithm can be applied to complex urban environments. To achieve these aims, the new heuristic diffraction model is embedded into an existing image based 3-D ray tracing model [12]. The modified model was then used in a path loss prediction comparison using outdoor measurements for the city of Bristol. The data was captured at 1.92 GHz and a full description of the channel sounder and its operating parameters is given in [13]. The Tx was mounted on a building roof-top (approx. 30 m from the ground) and 400 Rx points were placed along the measurement routes (approx. 1.7 m from the ground) as shown in Fig. 3. Prediction data was generated for both the heuristic and vertical plane diffraction models [3], [6]. For both cases, up to 4 orders of reflection and 2 orders of diffraction were considered. The results are shown in Fig. 4 and summarized in Table II.

A mean path loss error improvement of approximately 1 dB is seen when the heuristic algorithm is applied to determine the 3-D diffraction paths (relative to the vertical plane approach). Improvements in the standard deviation and the route correlation are also observed.

V. CONCLUSION

Simple solutions for multiple arbitrary edge diffraction using a geometrical approach are not present in the literature for image-based ray models. An algebraic approach involving a complex non-linear solution is too costly for application in detailed ray models. The heuristic geometric approach presented here is easy to implement and provides accurate ray paths for the vast majority of cases. The method overcomes the disadvantage of most image based ray tracing models, where rooftop diffraction is omitted or restricted to the same diffraction plane. This limitation can be significant, especially in outdoor propagation studies. Comparison with measurement data has shown that a significant improvement can be achieved when our new approach is used instead of traditional vertical plane diffraction.

REFERENCES

[1] G. E. Athanasiadou, A. R. Nix, and J. P. McGeehan, "A microcellular ray-tracing propagation model and evaluation of its narrow-band and wide-band predictions," *IEEE J. Select. Areas Commun.*, vol. 18, no. 3, pp. 322–335, Mar. 2000.

[2] D. A. McNamara, C. W. I. Pistorius, and J. A. G. Malherbe, *Introduction to the Uniform Geometrical Theory of Diffraction*. Norwood, MA: Artech House, 1990.

[3] G. Liang and H. L. Bertoni, "A new approach to 3-D Ray Tracing for propagation prediction in cities," *IEEE Trans. Antennas Propag.*, vol. 46, no. 6, 1998.

[4] D. B. Davidson, I. P. Theron, U. Jakobus, F. M. Landstorfer, F. J. C. Meyer, J. Mostert, and J. J. Van Tonder, "Recent progress on the antenna simulation program FEKO," in *Proc. Communications and Signal Processing*, Rondebosch, South Africa, Sep. 1998.

[5] F. Agelet, A. Formella, J. M. Rabanos, F. Vicente, and F. Fontan, "Efficient ray-tracing acceleration techniques for radio propogation modeling," *IEEE Trans. Veh. Tech.*, vol. 49, pp. 2089–2104, Nov. 2000.
[6] K. Rizk, R. Valenzuela, S. Fortune, D. Chizhik, and F. Gardiol, "Lateral, full 3-D and vertical plane propagation in microcells and small cells," in *Proc. IEEE 48th Vehicular Tech. Conf.*, May 1997, vol. 2, pp. 998–1003.
[7] T. Imai and T. Fujii, "Propagation loss in multiple diffraction using ray-tracing," in *IEEE Antennas and Propagation Society Int. Symp.*, Jul. 1997, vol. 4, pp. 2572–2575.
[8] E. Di Giampaolo and F. Bardati, "Analytical model of multiple wedge-diffracted ray congruence," *Electromagn.*, vol. 6, 2003.
[9] M. Toeltsch, J. Laurila, K. Kalliola, A. F. Molisch, P. Vainikainen, and E. Bonek, "Statistical characterization of urban spatial radio channels," *IEEE J. Select. Areas Commun.*, vol. 20, no. 3, Apr. 2002.
[10] J. Li, J. F. Wagen, and E. Lachat, "Propagation over rooftop and in the horizontal plane for small and micro-cell coverage predictions," in *Proc. IEEE 47th Vehicular Tech. Conf.*, May 1997, pp. 1123–1127.
[11] T. W. Ang, S. Y. Tan, and H. S. Tan, "Analytical methods to determine diffraction points on multiple edges and cylindrical scatterers in UTD ray tracing," *Microw. Opt. Tech. Letter*, vol. 22, no. 5, Sep. 1999.
[12] K. H. Ng, E. Tameh, and A. R. Nix, "An advanced multi-element microcellular ray tracing model," in *Proc. IEEE 1st Int. Symp. Wireless Communication Systems*, Mauritius, Sep. 20–24, 2004.
[13] S. E. Foo, M. A. Beach, P. Karlsson, P. Eneroth, B. Lindmark, and J. Johansson, "Spatio-temporal investigation of UTRA FDD channels," in *Proc. Inst. Elect. Eng. 3G Mobile Communication Technologies*, 2002, pp. 175–179.

E-Pulse Diagnostics of Curved Coated Conductors With Varying Thickness and Curvature

Jonathan F. Wierzba and Edward J. Rothwell

***Abstract*—The use of the E-pulse technique to diagnose changes in the material parameters of a coating on a conducting surface is examined. To include the effects of varying curvature and coating thickness, the canonical problem of an elliptical cylinder coated with a circular dielectric layer is considered. It is shown that E pulses created using the natural resonance frequencies of a planar coated conductor may be used in the diagnosis, as long as the thickness of the planar coating is taken to be equal to the thickness of the coating on the elliptical cylinder at the specular point. The performance of the E-pulse technique improves as the size of the cylinder is increased, since the curvature of the surface approaches that of a plane.**

***Index Terms*—Electromagnetic reflection, electromagnetic transient scattering, materials testing, nonhomogeneous media.**

I. Introduction

Material coatings are often applied to the conducting surfaces of air vehicles to reduce their radar cross section. The performance of these materials may deteriorate over time due to environmental conditions or improper repairs, and so the diagnosis of the electromagnetic health of the materials is crucial for successful maintenance. Recently, tools have been developed that use time-domain pulses to interrogate the material coatings. Information that is directly available in the transient scattered field may be incorporated into algorithms to assess the health of the structure [1].

Manuscript received December 1, 2005; revised May 19, 2006.

The authors are with the Department of Electrical and Computer Engineering, Michigan State University, East Lansing, MI, 48824 USA (e-mail: rothwell@egr.msu.edu).

Digital Object Identifier 10.1109/TAP.2006.880786

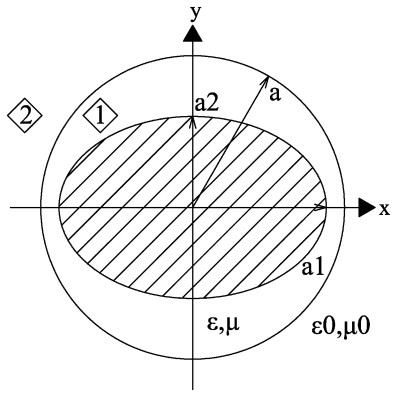

Fig. 1. Elliptical conductor with circular dielectric coating. Major axis is x-axis.

It has been shown that for planar coated conductors, the E-pulse method provides a simple means for diagnosis when the transient reflected-field response is available, since the multiple reflections of the waves within the coating comprise a natural mode series [2], [3]. Since the surfaces of air vehicles have many curved components, the extension of the E-pulse method to a coated surface with constant curvature and coating thickness was considered in [4]. There it was shown that while the field reflected by the coated curved surface is not a pure natural mode series, an E pulse created for a planar surface with the same coating thickness is useful for diagnosing changes to the curved coated conductor.

In this letter, application of the E-pulse technique to a curved coated conductor with varying curvature and coating thickness is considered by examining a conducting elliptical cylinder coated with a circular layer of dielectric material [5]. It is shown that again an E-pulse created for a planar coated conductor is useful for diagnosing changes to the material properties of the coating. In this case, the thickness of the planar coating is taken to be that of the cylinder coating at the specular point (the point on the coating surface where the direction of the incident plane wave is normal to the surface).

II. Calculation of the Scattered Field

Consider an elliptical conducting cylinder coated by a circular dielectric layer of radius a, permittivity ϵ and permeability μ, and immersed in free space, as shown in Fig. 1. In this figure the major axis of the ellipse is the x-axis, but the major axis may also be chosen as the y-axis. In each case, the semi-axis length along the x-axis is denoted as a_1 and along the y-axis as a_2. The fields will be described in circular-cylindrical coordinates (r, ϕ).

A plane wave is incident on the coated cylinder from $x > 0$ with its direction of propagation along the x-axis. Thus, there is symmetry of the fields about the x-axis. The polarization is denoted as TM_z when the incident electric field has only a $z$component, and TE_z when the incident magnetic field has only a z-component. For the case in which the x-axis is the major axis of the ellipse, the coating is thinnest at the specular point, and increases in thickness away from this point. For the case in which the y-axis is the major axis of the ellipse, the coating is thickest at the specular point, and decreases in thickness away from this point.

The field scattered by the coated cylinder is computed by expanding the fields in the coating layer and in the free-space background as a series of cylinder functions, applying the boundary conditions at $r = a$,